Available online at www.sciencedirect.com
ScienceDirect
Journal of Catalysis 245 (2007) 392–400
JOURNAL OF CATALYSIS
www.elsevier.com/locate/jcat

Specific performance of silica-coated Ni catalysts for the partial oxidation of methane to synthesis gas

Sakae Takenaka [a,*], Hiroshi Umebayashi [a], Eishi Tanabe [b], Hideki Matsune [a], Masahiro Kishida [a,*]

[a] *Department of Chemical Engineering, Graduate School of Engineering, Kyushu University, 744 Moto-oka, Nishi-ku, Fukuoka 819-0395, Japan*
[b] *Western Hiroshima Prefecture Industrial Institute, Kagamiyama, Higashi-Hiroshima, Hiroshima 739-0046, Japan*

Received 19 September 2006; revised 7 November 2006; accepted 7 November 2006

Available online 30 November 2006

Abstract

Silica-supported Ni catalysts were prepared by using water-in-oil typed microemulsion. By preparation using the microemulsion, Ni metal particles with diameters < ca. 5 nm were covered uniformly with silica layers with thickness of ca. 10 nm, whereas Ni metal particles were supported on the outer surface of silica by a conventional impregnation method. The Ni metal covered with silica (coat-Ni) showed excellent catalytic performance for the partial oxidation of methane into synthesis gas. Coat-Ni showed a high activity and a long life for the partial oxidation of methane at temperatures above 973 K to form CO and hydrogen, whereas Ni metal catalyst supported on silica was rapidly deactivated for the reaction. Ni *K*-edge XANES/EXAFS and temperature-programmed reduction for these catalysts showed that Ni metal particles in coat-Ni strongly interacted with silica. The strong interaction of Ni metal particles with silica would improve their catalytic performance for the partial oxidation of methane into synthesis gas.

Keywords: Silica-coated Ni catalyst; Silica-supported Ni catalyst; Microemulsion; Partial oxidation of methane

1. Introduction

Synthesis gas is industrially produced through the steam reforming of methane. However, the steam reforming of methane requires temperatures above 1000 K, as well as a large energy input due to a highly endothermic reaction. Thus, the production of synthesis gas through the partial oxidation of methane is of a current interest, because the reaction is an exothermic one [1,2]. The partial oxidation of methane produces synthesis gas of H_2/CO ratio = 2, whereas the H_2/CO ratio for the steam reforming of methane is 3. The H_2/CO ratio equal to 2 is suitable for the synthesis of methanol and higher hydrocarbons. Ni metal or noble metals, such as Pt and Rh, are often used as catalytically active components for the partial oxidation of methane [1–4]. Many research groups have developed various Ni catalysts effective for the reaction because of a high cost of noble metals [5–11]. Supported Ni catalysts show high activity for the partial oxidation of methane at temperatures above 1000 K. However, the life of Ni catalysts is not always so long. The deactivation of supported Ni catalysts resulted from the sintering of Ni metal particles, deposition of carbons, and oxidation of Ni metal [2,3,12,13]. Fine Ni metal particles supported on catalytic supports showed high activity for the partial oxidation of methane, but the catalytic activity decreased gradually during the reaction due to the sintering of Ni metal particles and/or the oxidation of the metal. In addition, aggregated Ni metal particles preferentially formed filamentous carbons during the partial oxidation of methane, whereas fine Ni metal particles were sustainable to carbon deposition [14–16]. The formation of filamentous carbons caused the stoppage of reactant gases, as well as the deactivation of catalysts. Therefore, the sintering of Ni metal particles during the partial oxidation of methane should be suppressed. To keep the size of Ni metal particles small during the reaction, a particular metal oxide that strongly interacts with Ni metal is usually used as a support of Ni catalysts, such as Ni/MgO and Ni/Al_2O_3 [8,9,17,18].

We have prepared silica-coated metal catalysts by using water-in-oil microemulsions and examined the catalytic perfor-

* Corresponding authors. Fax: +81 92 802 2752.
E-mail address: takenaka@chem-eng.kyushu-u.ac.jp (S. Takenaka).

0021-9517/$ – see front matter
doi:10.1016/j.jcat.2006.11.005

mance of the catalysts thus obtained [19–21]. By the preparation of catalysts using microemulsion, the metal particles could be coated uniformly with porous silica. The silica-coated metal catalysts are resistant to the sintering of metal particles during the catalytic reactions at high temperatures, because the metal particles are covered with silica. In general, it is recognized that Ni metal catalysts supported on silica showed poor activity for the partial oxidation of methane into synthesis gas [22,23]. This would be due to the sintering of Ni metal particles during the reactions at high temperatures, because chemical interaction of silica with Ni metals is weak [24]. However, Ni metal particles coated with silica would be resistant to sintering during the partial oxidation of methane.

In the present study, we prepared silica-coated Ni catalysts using microemulsion and characterized the catalysts by transmission electron microscopy (TEM), Ni *K*-edge X-ray absorption near-edge structure/extended X-ray absorption fine structure (XANES/EXAFS) and temperature-programmed reduction (TPR). In addition, the silica-coated Ni was used as the catalyst for the partial oxidation of methane into synthesis gas. We would report the superior performance of silica-coated Ni catalysts for the partial oxidation of methane.

2. Experimental

2.1. Preparation of catalysts

Ni catalysts coated with silica (denoted as coat-Ni hereafter) were prepared by using water-in-oil microemulsion. The microemulsion system was prepared by adding 5 mL of aqueous $Ni(NO_3)_2$ (1.0 M) into 100 mL of surfactant solution in cyclohexane (0.5 M). Polyoxyethylene ($n = 15$) cetyl ether was used as a surfactant. Nanoparticles of some compound containing Ni cations were synthesized by adding 6 mL of hydrazine ($N_2H_4{\cdot}H_2O$) in the microemulsion system. Hydrolysis and polycondensation of tetraethyl orthosilicate (TEOS) were performed at 323 K by adding 20 g of TEOS and 15 mL of aqueous NH_3 (1 M) into the microemulsion system. The precipitates thus obtained were washed with isopropanol several times after filtration and calcined at 773 K for 2 h under air stream. The calcined samples were washed with aqueous HNO_3 (1.0 M) at room temperature to remove Ni species that were not covered with silica layers. After this treatment, Ni loading for this sample was estimated by X-ray fluorescence spectroscopy (XRF). Silica-supported Ni catalysts (denoted as imp-Ni hereafter) were also prepared with a conventional impregnation method. The silica supports were prepared similarly to the preparation of coat-Ni. These catalyst samples were pressed into disks and crushed into 16–28 mesh size before the reaction test.

2.2. Partial oxidation of methane

Partial oxidation of methane into synthesis gas was performed at atmospheric pressure with a conventional gas flow system with a fixed catalyst bed. The catalyst samples diluted with quartz sands were packed in a tubular reactor made from quartz (length, 300 mm; i.d., 8 mm). Before the reaction, the catalysts were oxidized with oxygen at 973 K for 30 min and subsequently reduced with hydrogen at 973 K for 1 h. After the pretreatment of the catalysts, a mixed gas of methane and O_2 diluted with Ar was contacted with the catalysts at required temperatures (973–1073 K). During the reactions, a part of effluent gases from catalyst bed was sampled out and analyzed by on-line gas chromatography.

2.3. Characterization of catalysts

Measurement of XANES/EXAFS spectra was performed on the beamline BL 7C at Photon Factory in the Institute of Materials Structure Science for High-Energy Accelerator Research Organization, Tsukuba, Japan (proposal 2005G194). Ni *K*-edge XANES/EXAFS spectra of coat-Ni and imp-Ni were measured with a transmission mode with a Si(111) two-crystal monochromator at room temperature with a ring energy of 2.5 GeV and a stored current of 250–450 mA. To estimate the structures of Ni species in coat-Ni and imp-Ni catalysts before and after the partial oxidation of methane, the catalysts were treated under the following conditions before the measurement of Ni *K*-edge XANES/EXAFS. The catalysts that had been reduced with hydrogen at 973 K were contacted with a mixed gas of methane and oxygen diluted with Ar at 973 K. The reactor packed with the catalyst samples was cooled quickly from 973 K to room temperature when the catalysts were active or were deactivated completely for the reaction. After these treatments, the catalysts were packed into a polyethylene bag under Ar. The analysis of EXAFS data was performed by using an EXAFS analysis program, REX (Rigaku Co.). The Fourier transformation of k^3-weighted EXAFS oscillation was performed over the range of $k = 3.5$–15.5 Å^{-1}. Inversely Fourier-transformed data for each Fourier peak were analyzed by a curve-fitting method, using phase-shift and amplitude functions derived from EXAFS spectrum of Ni foil. TEM images of coat-Ni and imp-Ni were measured with a JEOL JEM-3000F.

TPR spectra for coat-Ni and imp-Ni were measured with a BELCAT (BEL Japan Inc.). Before the measurement of TPR spectra, coat-Ni and imp-Ni were oxidized with oxygen at 973 K for 1 h. The catalyst samples were heated from 373 to 973 K by a rate of 10 K min^{-1} under hydrogen stream.

3. Results and discussion

3.1. Characterization of coat-Ni catalysts

Fig. 1 shows TEM images of coat-Ni and imp-Ni. Both the samples were reduced with hydrogen at 973 K before the measurement of TEM images. Many spherical particles with diameters of 20–50 nm and darker spots with diameters of 2–5 nm were observed in the TEM images of both the catalysts. The darker spots in coat-Ni could be always observed in the center of the spherical particles, whereas those in imp-Ni seemed to be present on the surface of the spherical particles. As described below, the darker spots and the spherical particles observed in the TEM images were assignable to Ni metal particles and silica

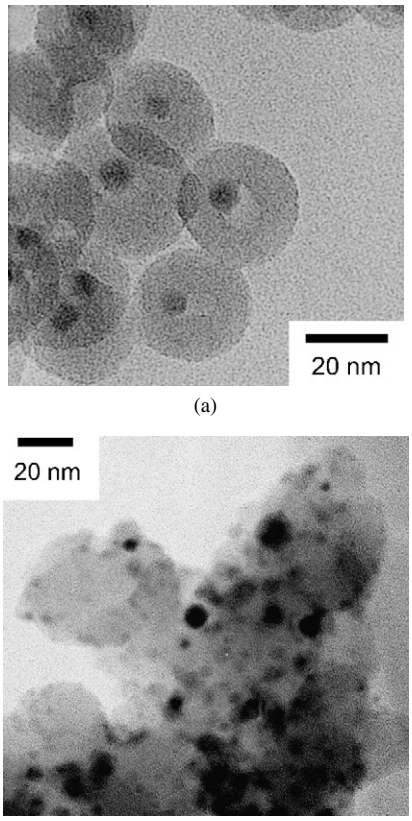

Fig. 1. TEM images of (a) coat-Ni and (b) imp-Ni.

particles, respectively. These results indicated that a Ni metal particle in coat-Ni was uniformly covered with silica layers, whereas those in imp-Ni were supported on the outer surface of spherical silica particles. It should be noted that Ni metal particles in coat-Ni were more monodispersed and smaller (<5 nm) than those in imp-Ni (5–10 nm). Before measurement of the TEM images, these catalysts were treated with hydrogen at 973 K. It is likely that Ni metal particles in coat-Ni were resistant to the sintering during the reduction with hydrogen at 973 K.

The loading of Ni for coat-Ni which had been washed with aqueous HNO_3 was estimated to be 3.4 wt% with XRF, while the loading for coat-Ni before washing with aqueous HNO_3 was 5.1 wt%. On the other hand, Ni loading for imp-Ni was estimated to be 3.9 wt%, but the Ni species in imp-Ni were completely removed by washing with aqueous HNO_3. These results also suggest that Ni metal particles in coat-Ni catalysts were covered uniformly with silica layers.

Fig. 2 shows Ni K-edge XANES spectra of coat-Ni, imp-Ni, Ni foil, and NiO (average crystallite size, ca. 50 nm). Ni K-edge XANES and EXAFS of coat-Ni and imp-Ni catalysts were measured after reduction with hydrogen at 973 K. The XANES spectrum of Ni foil was different from that of NiO in shape. In general, XANES spectra of any metal species are sensitive to their electronic states and local structures [25–28]. The Ni K-edge XANES spectrum for imp-Ni was consistent with that for Ni foil, indicating that Ni species in imp-Ni were present mainly as Ni metal. On the other hand, the XANES spectrum

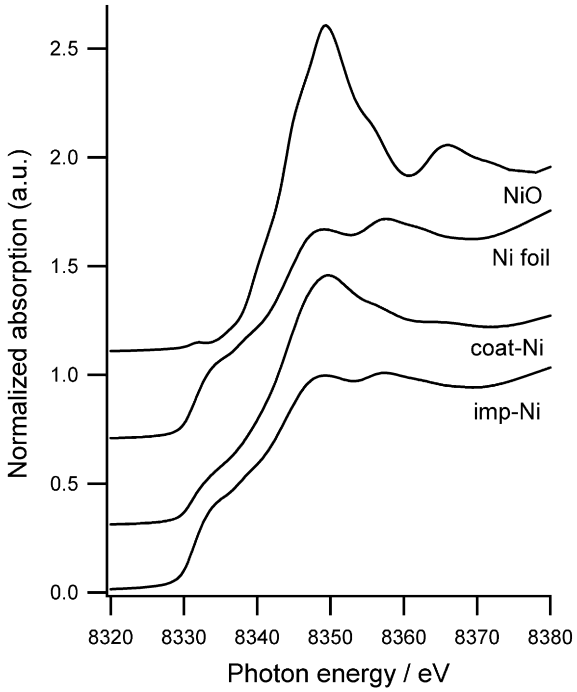

Fig. 2. Ni K-edge XANES spectra of imp-Ni, coat-Ni, Ni foil and NiO.

for coat-Ni did not coincide with that for Ni foil or that for NiO. In the XANES spectrum of coat-Ni, a shoulder peak characteristic of the spectrum for Ni foil was observed at 8333 eV. In addition, a sharp peak characteristic of the spectrum for NiO was confirmed at 8348 eV in the spectrum of coat-Ni, although the intensity of the peak for coat-Ni was significantly lower than that for NiO. These results imply that some parts of Ni metal particles in coat-Ni were oxidized even after the reduction with hydrogen at 973 K for 1 h. As shown in Fig. 1, small Ni metal particles in coat-Ni were completely covered with silica layers, whereas those in imp-Ni were stabilized on the outer surface of silica. The silica layers that wrapped Pt metal particles in coat-Ni were composed of many primary particles of silica. The primary particles of silica were contacted directly with the surface of Ni metal particles in coat-Ni. Thus, many Ni atoms present on the surface of the metal particles in coat-Ni interacted directly with silica, whereas some of them in imp-Ni contacted with silica. Ni metal particles in coat-Ni likely were partly oxidized, because many Ni atoms on the surface of the metal particles interacted directly with silica through Si–O–Ni bonds.

Fig. 3 shows Ni K-edge k^3-weighted EXAFS spectra of coat-Ni, imp-Ni, Ni foil, and NiO. The feature of EXAFS oscillation for Ni foil was different from that for NiO. EXAFS spectra for coat-Ni and imp-Ni were similar to that for Ni foil. Thus, Ni species in coat-Ni and imp-Ni were present mainly as Ni metal. As described earlier, the XANES spectrum of coat-Ni suggested that Ni metal particles in coat-Ni were partly oxidized. The peak at 8348 eV in the XANES spectrum of NiO was significantly more intense than the other peaks in the XANES spectra of NiO and Ni foil, as shown in Fig. 2. Thus, even if the fraction of NiO to all of the Ni species in the catalysts was very small, the peak due to NiO at 8348 eV could be ob-

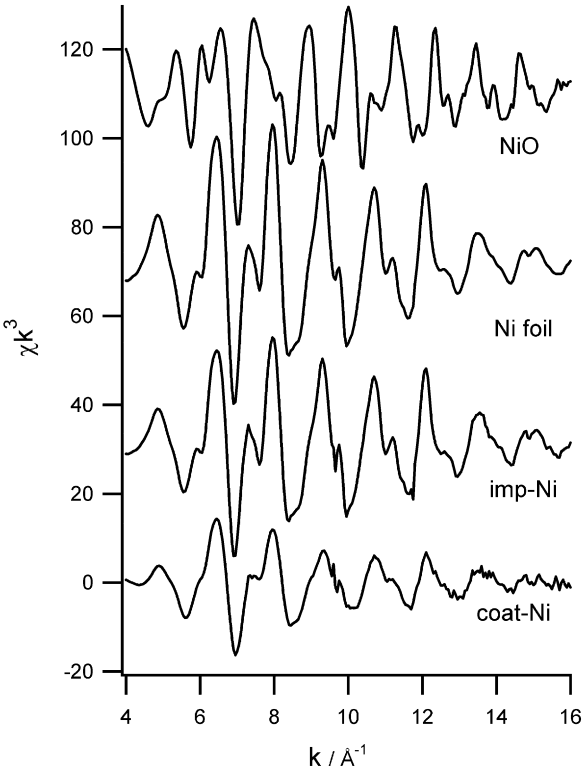

Fig. 3. Ni K-edge k^3-weighted EXAFS spectra of imp-Ni, coat-Ni, Ni foil and NiO.

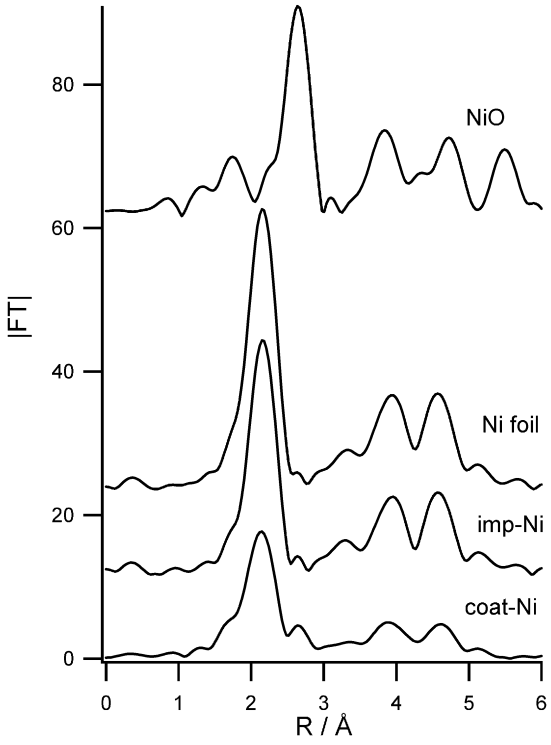

Fig. 4. Fourier transforms of Ni K-edge k^3-weighted EXAFS spectra of imp-Ni, coat-Ni, Ni foil and NiO.

served in the XANES spectrum. Taking the XANES/EXAFS spectra of coat-Ni into consideration, the fraction of oxidized Ni species to all the Ni species in coat-Ni would be small. The EXAFS oscillations in Fig. 3 were stronger in the order of Ni foil > imp-Ni > coat-Ni. The intensity of the EXAFS oscillation corresponds to an average crystallite size of Ni metal [29]. Thus, an average crystallite size of Ni metal in coat-Ni was smaller than that in imp-Ni. This result is consistent with that of TEM images shown in Fig. 1.

Fig. 4 shows Fourier transforms of Ni K-edge EXAFS spectra (radial structure functions [RSFs]) for coat-Ni, imp-Ni, Ni foil, and NiO. In the RSF for Ni foil, a strong peak was observed at 2.1 Å. The peak is assignable to the back-scattering from the first neighboring Ni atoms in Ni metal. In the RSF for NiO, the peaks due to Ni–O and due to Ni–Ni bonds were observed at around 1.7 and 2.8 Å, respectively. The features of RSFs for imp-Ni and coat-Ni are very similar to that for Ni foil. In the RSF for coat-Ni, peaks due to Ni–O could not be observed at around 1.7 Å, whereas the XANES spectrum showed that Ni metal particles in this catalyst were partly oxidized. Thus, the fraction of oxidized Ni species to all the Ni species in coat-Ni was small. The intensity of the peak due to Ni–Ni at 2.1 Å in the RSF of coat-Ni was smaller than that of imp-Ni. Generally speaking, the peak intensity due to metal–metal bonds in the RSFs for any metals becomes stronger with crystallite sizes of the metal [29]. In order to estimate the structural parameters of Ni metal (the coordination number and interatomic distance for Ni–Ni bonds) in these catalysts, curve-fitting analyses were performed for the peak at around 2.1 Å in the RSFs, on the basis of the interatomic distance = 2.49 Å and the coordination number = 12 for Ni–Ni bonds in Ni foil. Both the EXAFS spectra for coat-Ni and imp-Ni could be fitted by a shell of Ni–Ni bond. The coordination number and interatomic distance of Ni–Ni bonds were evaluated to be 6.5 and 2.47 Å for coat-Ni, and 9.2 and 2.49 Å for imp-Ni, respectively. These results indicated that the average size of Ni metal crystallites for coat-Ni was smaller than that in imp-Ni. It should be noted that Ni loading of coat-Ni (3.4 wt%) was almost the same as that of imp-Ni (3.9 wt%). These catalysts were reduced with hydrogen at 973 K before the measurements of Ni K-edge XANES/EXAFS and TEM images. Ni metal particles in imp-Ni may be aggregated to form larger ones during the reduction with hydrogen. Each Ni metal particle in coat-Ni was completely covered with silica, which must prevent the sintering of the metal particles during the reduction with hydrogen.

Fig. 5 shows the pore size distribution for silica layers in coat-Ni. This result was evaluated by the adsorption of Ar on coat-Ni at 87 K. As shown in Fig. 5, the silica layers that wrapped Ni metal particles had a pore structure with diameters <2 nm. The silica layers in coat-Ni were composed of many primary silica particles. The aggregates of small silica particles would form micropores with diameters <2 nm. Therefore, when coat-Ni is used as the catalyst for the partial oxidation of methane, reactant molecules can be diffused in the silica layers to contact with Ni metal particles.

3.2. Partial oxidation of CH_4 over the catalysts

Fig. 6 shows the changes of methane conversion (a) and selectivity to CO (b) with time on stream during the partial

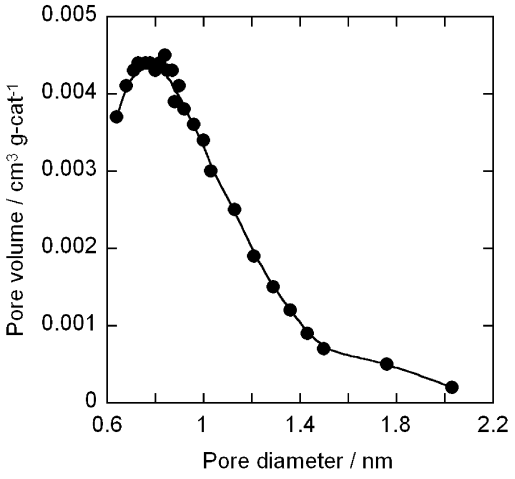

Fig. 5. Pore size distribution for silica layers in coat-Ni.

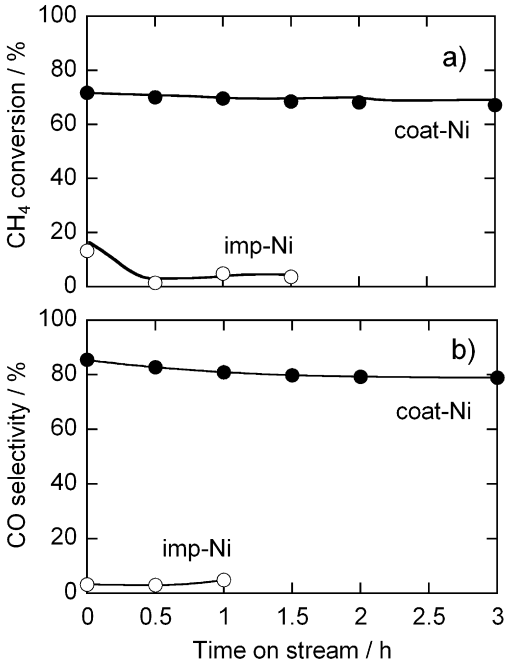

Fig. 6. Change of methane conversion (a) and selectivity to CO (b) with time on stream in the partial oxidation of methane over coat-Ni and imp-Ni at 973 K. Catalyst weight = 0.10 g, $P(CH_4) = 36.8$ kPa, $P(O_2) = 18.4$ kPa, flow rate = 110 ml min^{-1}.

oxidation of methane at 973 K over coat-Ni and imp-Ni catalysts. In the reaction test over imp-Ni catalyst, the conversion of methane and selectivity to CO were very low, because the total oxidation of methane into CO_2 and H_2O proceeded preferentially over the catalyst. As described earlier, Ni species in imp-Ni before the reaction were present as Ni metal, which was catalytically active species for the partial oxidation of methane. Imp-Ni would be quickly deactivated for the partial oxidation of methane into synthesis gas after the contact with methane and oxygen. In contrast, coat-Ni catalyst showed high activity for the partial oxidation of methane. Hydrogen, CO, and CO_2 were formed in the reaction over coat-Ni catalyst. The conversion of methane and selectivity to CO over coat-Ni catalyst were significantly higher than those over imp-Ni. In addition, coat-

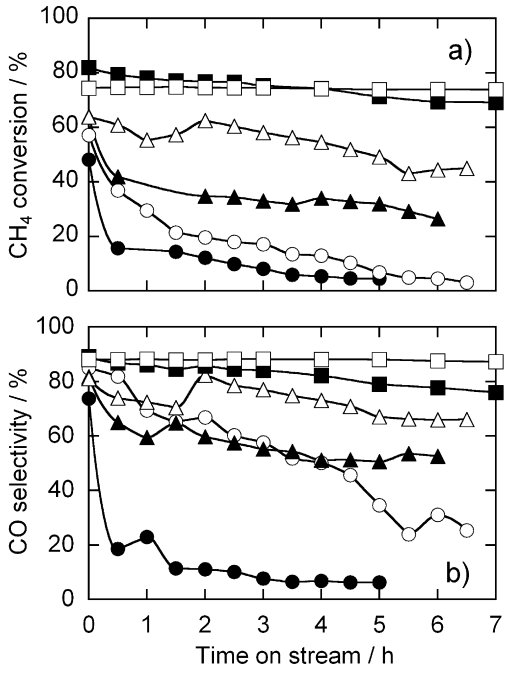

Fig. 7. Effect of W/F values on the methane conversion (a) and selectivity to CO (b) in the partial oxidation of methane at 973 K over coat-Ni catalysts. $W/F = 1.8 \times 10^{-4}$ (●), 3.0×10^{-4} (○), 4.5×10^{-4} (▲), 13.6×10^{-4} (△), 36.4×10^{-4} (■) and 54.5×10^{-4} g_{cat} min ml^{-1} (□). $P(CH_4) = 36.8$ kPa, $P(O_2) = 18.4$ kPa, catalyst = 0.03–0.30 g.

Ni catalyst retained high activity and high selectivity to CO for 3 h of time on stream. These results indicated that coat-Ni catalyst showed superior performance for the partial oxidation of methane to imp-Ni. Many research groups have examined the effect of supports for Ni metal on the partial oxidation of methane [1–3,13,30]. According to these studies, MgO and Al_2O_3 were suitable supports for Ni, because the strong interaction of Ni metal with these supports prevented sintering of the metal during the reaction. In contrast, Ni metal particles supported on silica were easily aggregated due to their weak interaction during the catalytic reactions [24]. The present study showed that coat-Ni catalysts (i.e., Ni metal particles uniformly covered with silica layers) are effective ones for the partial oxidation of methane. The coverage of Ni metal with silica layers would result in a change in the chemical property of Ni metal, as well as high sustainability to sintering of the metal particles.

Fig. 7 shows the change in methane conversion and selectivity to CO with time on stream over coat-Ni catalysts at 973 K. These reaction tests were carried out under different W/F values. W/F values changed from 1.8×10^{-4} to 5.5×10^{-3} g_{cat} min ml^{-1}. As W/F values increased from 1.8×10^{-4} to 3.6×10^{-3}, the conversion of methane and selectivity to CO at early period of the reaction increased. In addition, the deactivation of coat-Ni for the partial oxidation of methane also depended on the W/F values. The methane conversion and selectivity to CO were maintained to high levels in the reactions of W/F values $>36.4 \times 10^{-4}$, whereas the catalytic activity rapidly decreased early in the reaction tests with W/F values of 1.8×10^{-4} to 4.5×10^{-4}.

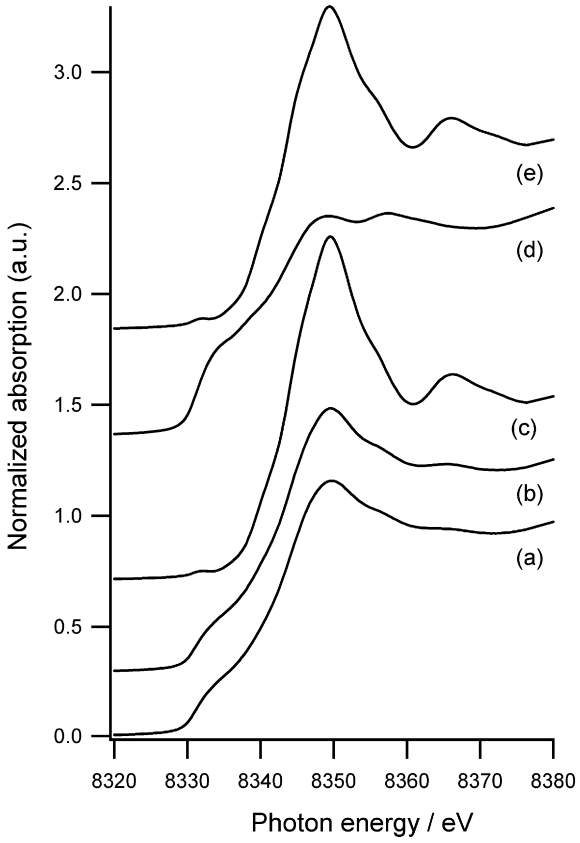

Fig. 8. Ni K-edge XANES spectra of coat-Ni and imp-Ni before and after the partial oxidation of methane at 973 K. (a) coat-Ni before the reaction; (b) coat-Ni after the reaction (active catalyst); (c) coat-Ni after the deactivation; (d) imp-Ni before the reaction; (e) imp-Ni after the deactivation.

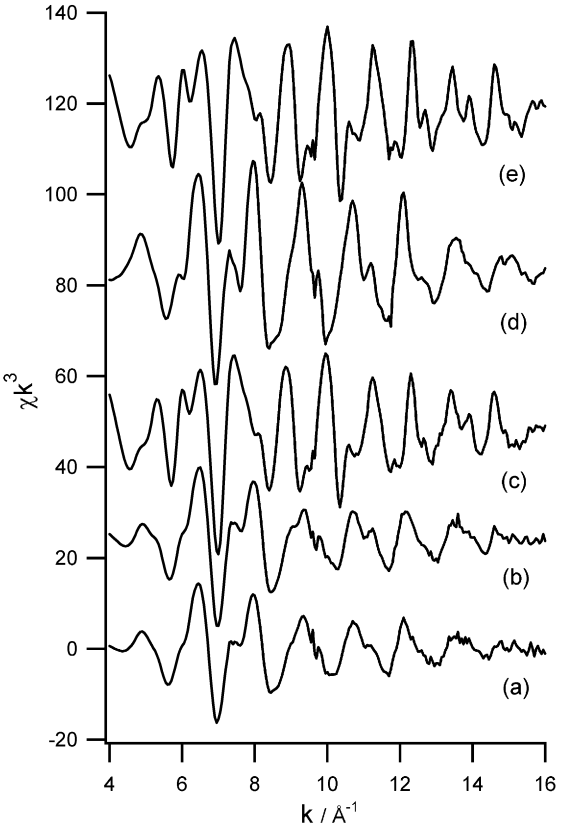

Fig. 9. Ni K-edge k^3-weighted EXAFS spectra of coat-Ni and imp-Ni before and after the partial oxidation of methane at 973 K. (a) coat-Ni before the reaction; (b) coat-Ni after the reaction (active catalyst); (c) coat-Ni after the deactivation; (d) imp-Ni before the reaction; (e) imp-Ni after the deactivation.

The deactivation of coat-Ni catalysts for the partial oxidation of methane in Fig. 7 may result from the oxidation of Ni metal. To clarify the state of Ni species in coat-Ni during the partial oxidation of methane, Ni K-edge XANES and EXAFS spectra for coat-Ni were measured. Fig. 8 shows Ni K-edge XANES spectra of coat-Ni and imp-Ni before and after the partial oxidation of methane at 973 K. XANES spectrum for coat-Ni, which showed high activity for the reaction [spectrum (b)], was similar to that of the catalyst before the reaction [spectrum (a)]. This result suggested that most Ni species in coat-Ni were present as Ni metal when the catalyst showed high activity for the partial oxidation of methane. In contrast, the XANES spectrum of coat-Ni was changed significantly after deactivation of the catalyst for the reaction. The XANES spectrum of coat-Ni after the complete deactivation [spectrum (c)] was very similar to that of NiO in Fig. 2. Thus, Ni species in coat-Ni were changed from Ni metal to NiO during deactivation for the reaction. The structural change of Ni species in imp-Ni was also investigated by Ni K-edge XANES. The XANES spectrum of imp-Ni after the deactivation [spectrum (e)] was compatible with that of NiO, whereas the spectrum of the catalyst before the reaction [spectrum (d)] was assignable to Ni metal. Therefore, the oxidation of Ni metal into NiO caused the deactivation of coat-Ni and imp-Ni for the partial oxidation of methane. As for the partial oxidation of methane over the Ni catalysts, it was proposed that part of methane reacted with O_2 to form CO_2 and H_2O at the upper part of catalyst bed, and then the remainder of methane reacted with CO_2 or H_2O to form synthesis gas at the lower part of catalyst bed [3,31]. The total oxidation of methane into CO_2 and H_2O was catalyzed by NiO, whereas the reforming of methane with CO_2 and H_2O into synthesis gas was catalyzed by Ni metal. Thus, when the W/F values were smaller in the partial oxidation of methane over the Ni catalysts, the total oxidation of methane would proceed preferentially, compared with the reforming of methane with CO_2 or H_2O. Therefore, coat-Ni catalyst would be deactivated more rapidly for the partial oxidation of methane as the W/F values decreased.

Ni K-edge EXAFS spectra for coat-Ni and imp-Ni also showed the oxidation of Ni metal in the catalysts after deactivation for the partial oxidation of methane. Fig. 9 showed Ni K-edge k^3-weighted EXAFS spectra of coat-Ni and imp-Ni before and after the partial oxidation of methane at 973 K. The EXAFS spectrum for the coat-Ni, which showed high activity for the reaction [spectrum (b)], was consistent with that for the catalyst before the reaction [spectrum (a)]. Thus, most Ni species in coat-Ni were present as Ni metal when coat-Ni catalyzed the partial oxidation of methane into synthesis gas. In contrast, the feature of EXAFS spectrum for coat-Ni changed after deactivation for the reaction. The spectrum [spectrum (c)] for the deactivated catalyst was quite similar to that of NiO shown in Fig. 3. The EXAFS spectra for imp-Ni also showed a

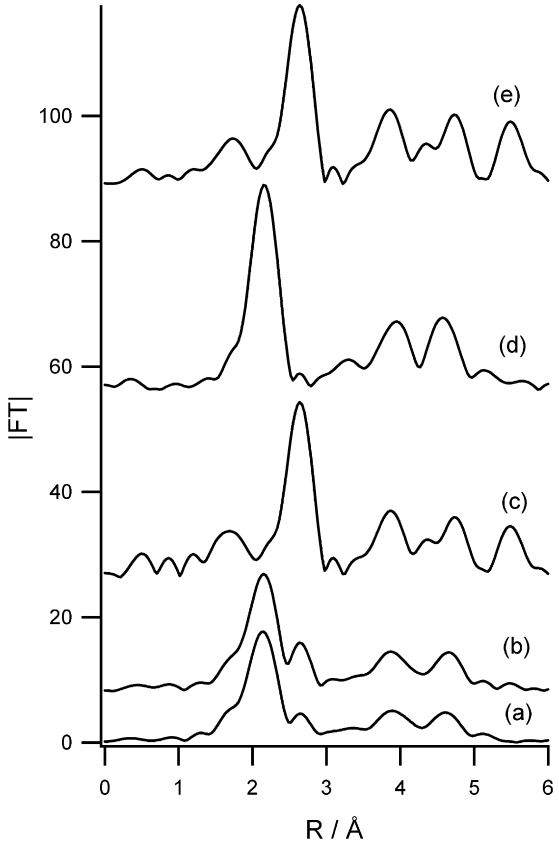

Fig. 10. Fourier transforms of Ni K-edge k^3-weighted EXAFS spectra of coat-Ni and imp-Ni before and after the partial oxidation of methane at 973 K. (a) coat-Ni before the reaction; (b) coat-Ni after the reaction (active catalyst); (c) coat-Ni after the deactivation; (d) imp-Ni before the reaction; (e) imp-Ni after the deactivation.

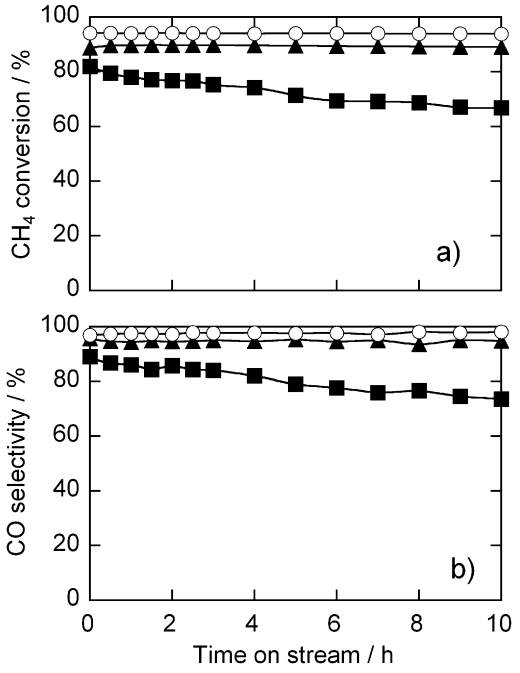

Fig. 11. Change of methane conversion (a) and selectivity to CO (b) with time on stream in the partial oxidation of methane over coat-Ni catalysts at different temperatures. Temperature = 973 (■), 923 (▲) and 1073 K (○). Catalyst = 0.20 g, $P(CH_4) = 36.8$ kPa, $P(O_2) = 18.4$ kPa, flow rate = 55 ml min^{-1}.

similar structural change of Ni species to that in coat-Ni; that is, Ni species in imp-Ni were changed from Ni metal to NiO after deactivation.

Fig. 10 shows Fourier transforms of k^3-weighed EXAFS spectra (RSFs) for coat-Ni and imp-Ni before and after the partial oxidation of methane at 973 K. In the RSF of coat-Ni, which showed high activity for the reaction [spectrum (b)], a strong peak due to Ni–Ni bonds in Ni metal was observed at 2.1 Å. However, this peak in the RSF disappeared after deactivation of coat-Ni, and new peaks appeared at 1.8 and 2.8 Å. The RSF for the deactivated coat-Ni was consistent with that of deactivated imp-Ni. The RSFs for the coat-Ni and imp-Ni after the deactivation could be assignable to NiO from the spectrum shown in Fig. 4. Thus, Ni species in coat-Ni and imp-Ni deactivated for the partial oxidation of methane were present as NiO. The oxidation of Ni metal to NiO resulted in deactivation of the catalysts for the reaction.

Carbon deposition on coat-Ni during the partial oxidation of methane should be taken into consideration as a factor in catalyst deactivation. Thus, the amount of carbon deposited on coat-Ni after complete deactivation for the partial oxidation of methane at 973 K was evaluated by thermogravimetric analysis. The deactivated coat-Ni was heated from room temperature to 973 K under air stream in thermogravimetric analysis. However, little change in the weight of the deactivated coat-Ni was observed. Thus, the deposition of carbons on coat-Ni during the partial oxidation of methane could be negligible. Generally, fibrous carbons were formed on the supported Ni catalysts during the partial oxidation of methane [32]. Ni metal particles on the supports decomposed methane into carbon and hydrogen, and the metal particles left the supports to form fibrous carbons [15,16,33,34]. Ni metal particles were present at the tip of the fibrous carbons, to decompose methane and grow the fibrous carbons. In coat-Ni, Ni metal particles did not have sufficient room to grow the fibrous carbons, because the metal particles were uniformly covered with silica. In addition, Ni metal particles in coat-Ni strongly interacted with silica, as described earlier. The strong interaction of Ni metal particles with silica should prevent detachment of the metal particles from silica. Thus, Ni metal particles in coat-Ni could not grow fibrous carbons from methane. These factors explain why coat-Ni catalysts were sustainable to carbon deposition during the partial oxidation of methane.

Fig. 11 shows the change of methane conversion (a) and selectivity to CO (b) with time on stream in the partial oxidation of methane over coat-Ni at different temperatures. Reaction temperatures were changed from 973 to 1073 K. Methane conversion attained ca. 80% at the early period of the reaction at 973 K but decreased gradually with time on stream. In addition, selectivity to CO also decreased with time on stream in the reaction at 973 K. This gradual deactivation of coat-Ni would be due to the oxidation of Ni metal. NiO catalyzed the total oxidation of methane [3,6], resulting in decreased selectivity to CO with time on stream. In contrast, the conversion of methane and selectivity to CO were maintained to high lev-

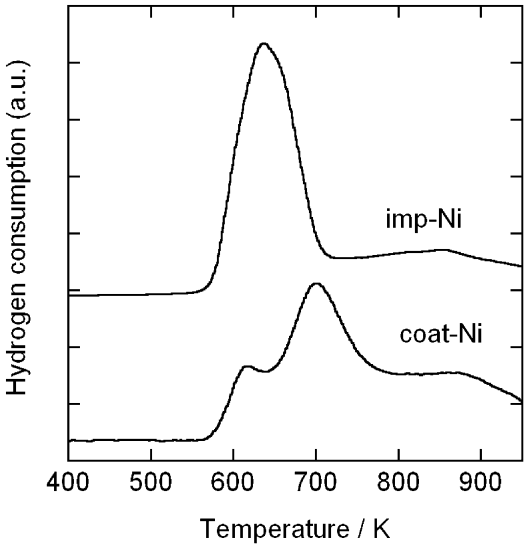

Fig. 12. TPR spectra of coat-Ni and imp-Ni.

els in the reactions at temperatures above 1023 K for 10 h time on stream. The compositions of hydrogen and CO in the effluent gases from the catalyst bed in the reactions at 1023 and 1073 K were very similar to the thermodynamic equilibrium values at the corresponding temperature. These results indicate that coat-Ni catalysts showed high and stable activity for the partial oxidation of methane.

The excellent catalytic performance of coat-Ni for the partial oxidation of methane may result from the change in chemical properties of Ni species due to the coverage with silica. Thus, TPR spectra of coat-Ni and imp-Ni were measured. The results are shown in Fig. 12. In the TPR spectrum for imp-Ni, a broad peak was observed at around 600 K. This peak was assigned to the reduction of NiO, which was weakly interacted with silica, into Ni metal on the basis of previous reports [9,24]. On the other hand, a peak at around 700 K was observed in addition to the peak at 600 K in the TPR spectrum of coat-Ni. In addition, the peak at around 700 K in the TPR spectrum of coat-Ni had a long tail toward higher temperatures. In the TPR spectrum of coat-Ni, the intensity of the peak at 700 K was significantly stronger than that of the peak at 600 K. These results indicate that at least two types of NiO species were present in coat-Ni catalysts. One type was NiO, which was weakly interacted with silica, based on the TPR spectrum of imp-Ni. The other was NiO species, which are more difficult to reduce with hydrogen than the former species. TPR studies on Ni/MgO and Ni/Al_2O_3 also showed the presence of NiO species that required higher temperatures for reduction with hydrogen than bulk NiO [12,18,22]. These NiO species were assignable to Ni–Mg–O solid solution in Ni/MgO and $NiAl_2O_4$ in Ni/Al_2O_3. It was proposed that these NiO species in Ni/MgO and Ni/Al_2O_3 were reduced with hydrogen to form small Ni metal particles, which showed high activity for the partial oxidation of methane. In addition, the Ni metal particles in Ni/MgO and Ni/Al_2O_3 were resistant to sintering due to the strong interaction with the supports. In the present study, the NiO species reduced at around 700 K in the TPR spectrum of coat-Ni would be assignable to those strongly interacted with silica. The XANES spectrum of coat-Ni also implied the strong interaction of NiO species with silica. It is likely that the Ni metal particles formed from the NiO species strongly interacted with silica in coat-Ni show high resistibility to sintering and oxidation during the partial oxidation of methane. The formation of this NiO species by the coverage with silica would improve the catalytic activity and life for the partial oxidation of methane.

4. Conclusion

Silica-coated Ni metal particles (coat-Ni) were prepared using microemulsion. The silica-coated Ni catalysts showed higher activity and longer life for the partial oxidation of methane into synthesis gas compared with silica-supported Ni catalysts. The Ni species in coat-Ni strongly interacted with silica, resulting in the formation of catalytically active sites effective for the partial oxidation of methane.

References

[1] S. Freni, G. Calogero, S. Cavallaro, J. Power Sources 87 (2000) 28.
[2] A.P.E. York, T. Xiao, M.L.H. Green, Top. Catal. 22 (2003) 345.
[3] D. Dissanayake, M.P. Rosynek, K.C.C. Kharas, J.H. Lunsford, J. Catal. 132 (1991) 117.
[4] D.A. Hickman, L.D. Schmidt, J. Catal. 138 (1992) 267.
[5] T. Hayakawa, H. Harihara, A.G. Andersen, K. Suzuki, H. Yasuda, T. Tsunoda, S. Hamakawa, A.P.E. York, Y.S. Yoon, M. Shimizu, K. Takehira, Appl. Catal. A Gen. 149 (1997) 391.
[6] F. van Looij, J.W. Geus, J. Catal. 168 (1997) 154.
[7] F. Basile, L. Basini, M. D'Amore, G. Fornasari, A. Guarinoni, D. Matteuzzi, G. Del Piero, F. Trifirò, A. Vaccari, J. Catal. 173 (1998) 247.
[8] H. Morioka, Y. Shimizu, M. Sukenobu, K. Ito, E. Tanabe, T. Shishido, K. Takehira, Appl. Catal. A Gen. 215 (2001) 11.
[9] T. Shishido, M. Sukenobu, H. Morioka, M. Kondo, Y. Wang, K. Takaki, K. Takehira, Appl. Catal. A Gen. 223 (2002) 35.
[10] K. Heitnes, S. Lindberg, O.A. Rokstad, A. Holmen, Catal. Today 24 (1995) 211.
[11] K. Takehira, T. Hayakawa, H. Harihara, A.G. Andersen, K. Suzuki, M. Shimizu, Catal. Today 24 (1995) 237.
[12] J. Requies, M.A. Cabrero, V.L. Barrio, M.B. Güemez, J.F. Cambra, P.L. Arias, F.J. Pérez-Alonso, M. Ojeda, M.A. Penâ, M.J.L. Fierro, Appl. Catal. A Gen. 289 (2005) 214.
[13] V.R. Choudhary, A.M. Rajput, A.S. Mamman, J. Catal. 178 (1998) 576.
[14] S. Takenaka, H. Ogihara, I. Yamanaka, K. Otsuka, Appl. Catal. A Gen. 217 (2001) 101.
[15] S. Takenaka, S. Kobayashi, H. Ogihara, K. Otsuka, J. Catal. 217 (2003) 79.
[16] O. Yamazaki, T. Nozaki, K. Omata, K. Fujimoto, Chem. Lett. (1992) 1953.
[17] J. Barbero, M.A. Peña, J.M. Compos-Martin, J.L.G. Fierro, P.L. Arias, Catal. Lett. 87 (2003) 211.
[18] Y. Chu, S. Li, J. Lin, J. Gu, Y. Yang, Appl. Catal. A Gen. 134 (1996) 67.
[19] M. Kishida, T. Tago, T. Hatsuta, K. Wakabayashi, Chem. Lett. (2000) 1108.
[20] M. Ikeda, T. Tago, M. Kishida, K. Wakabayashi, Chem. Commun. (2001) 2512.
[21] T. Tago, T. Hatsuta, K. Miyajima, M. Kishida, S. Tashiro, K. Wakabayashi, J. Am. Ceram. Soc. 85 (2002) 2188.
[22] V.R. Choudhary, B.S. Uphade, A.S. Mamman, J. Catal. 172 (1997) 281.
[23] V.R. Choudhary, A.M. Rajput, B. Prabhakar, A.M. Mamman, Fuel 77 (1998) 1803.
[24] S. Takenaka, E. Kato, Y. Tomikubo, K. Otsuka, J. Catal. 219 (2003) 176.
[25] S. Takenaka, T. Tanaka, Y. Yamazaki, T. Funabiki, S. Yoshida, J. Phys. Chem. B 101 (1997) 9035.

[26] S. Takenaka, T. Tanaka, T. Funabiki, S. Yoshida, J. Phys. Chem. B 102 (1998) 2960.
[27] T. Tanaka, H. Yamashita, R. Tsuchitani, T. Funabiki, S. Yoshida, J. Chem. Soc. Faraday Trans. 1 84 (1988) 2987.
[28] N.M.D. Brown, J.B. McMonagle, G.N. Greaves, J. Chem. Soc. Faraday Trans. 1 80 (1984) 589.
[29] R.B. Greegor, F.W. Lytle, J. Catal. 63 (1980) 476.
[30] W.J.M. Vermeiren, E. Blomsma, P.A. Jacobs, Catal. Today 13 (1992) 427.
[31] P.D.F. Vernon, M.L.H. Green, A.K. Cheetham, A.T. Ashcroft, Catal. Lett. 6 (1990) 181.
[32] J.B. Claridge, M.L.H. Green, S.C. Tsang, A.P.E. York, A.T. Ashcroft, P.D. Battle, Catal. Lett. 22 (1993) 299.
[33] J.R. Rostrup-Nielsen, J. Catal. 33 (1974) 184.
[34] H. Bartholomew, Catal. Rev. Sci. Eng. 24 (1982) 67.